J. BRAAKSMA, R. BABUŠKA, J.B. KLAASSENS AND C. DE KEIZER

A COMPUTATIONALLY EFFICIENT MODEL FOR PREDICTING OVERFLOW MIXTURE DENSITY IN A HOPPER DREDGER

ABSTRACT

Trailing suction hopper dredgers are primarily used in land reclamation projects. In such projects, the operators of the hopper dredger aim to achieve the highest production possible. This production depends on the incoming sand production and on the losses during the overflow phase. This article presents three models to predict these overflow losses. The first model is based on a piecewise linear approximation of the mixture density distribution. The second model is based on an exponential density distribution and the third model is based on a piecewise constant approximation of the mixture density distribution, the so-called water-layer model. The models will be used for an online optimisation system such as a model predictive controller. This application requires that for every controller sample time, the model be executed up to 1000 times. Therefore these models must be computationally fast and accurate. They are validated on data measured onboard a ship and in a laboratory test rig. The test rig data show that these models are able to predict the sand bed height as well as the overflow density. The ship data confirm that the best performing model is the water-layer model. All models are fast and simulate the dynamics of a whole dredging process of 1.5 hours in less than 0.2 second. The exponential and the water-layer model have similar accuracy for the training data, but the cross validation results show that the water-layer model is more accurate. This model is therefore chosen for the use in the online optimisation system. The linear model is not accurate enough and has been rejected.

This research is sponsored in part by Senter, Netherlands Ministry of Economic Affairs within the project Artificial Intelligence for the Control of a Hopper Dredger (grant no. TSMA 2017). Thanks go also to MTI Holland, especially S. C. Ooijens and A. de Gruiter, for supplying the data measured on the test rig the *Schanulleke*. Finally thanks go to IHC Systems for financial support and for helping to acquire the measured data.

Above, A trailing suction hopper dredger (TSHD) at work on a land reclamation project in Dubai. Such massive projects would not be economically feasible were it not for the high sand production of TSHDs. Achieving efficient incoming sand production and limiting sand losses during the overflow phase is essential.

INTRODUCTION

A trailing suction hopper dredger is sea-going vessel equipped with one or two suction pipes that excavate sand from the sea bottom. Attached to these pipes is a draghead which acts as a giant vacuum cleaner (Figure 1). In contrast to the stationary dredger, this vessel trails the dragheads over the bottom.

During dredging, a pump sucks up mixture of soil and water and transports it to a cargo hold called the hopper. There the heavy grains settle to the bottom of the hopper and form a sand bed. The hopper is equipped with two overflow pipes to discharge excess water. Once the height of the hopper content in the hopper reaches the height of these pipes, water and lightweight grains start flowing out.

As the sand bed grows, the density of the outgoing mixture increases, which leads to higher overflow losses. Although the physical behaviour of the grains causes some of the losses (the natural losses), the operating conditions, such as the pump speed and the change in overflow position, influence the rest of the losses.

JELMER BRAAKSMA
received his BSc and MSc in 2003 in electrical engineering from the Delft University of Technology (TU Delft), the Netherlands. He is currently employed at the Delft Center for Systems and Control, Mechanical Engineering Department, TU Delft where he is doing his PhD research on artificial intelligence for the trailing suction hopper dredger in cooperation with IHC Systems.

ROBERT BABUŠKA
received his MSc in control engineering from the Czech Technical University in Prague in 1990, where he was appointed to the faculty of the Technical Cybernetics Department. In 1997 he received a PhD from TU Delft, the Netherlands and was appointed to the Electrical Engineering Faculty there and is currently Professor at the Delft Center for Systems and Control, Mechanical Engineering Faculty. He is the chairman of the IFAC Technical Committee on Cognition and Control.

BEN KLAASSENS
received his BS, MS and PhD degrees in electrical engineering from TU Delft, the Netherlands, where he is currently associate professor at the Control Laboratory. He has published extensively on series-resonant converters for low and high power applications and has designed and built prototypes of the early DC-DC to AC-AC series-resonant converters for a wide variety of applications. His current interest is in Mechatronics and Robotics.

CEES DE KEIZER
graduated in 1975 from TU Delft, the Netherlands, Electrical Engineering Faculty, Control Laboratory. Since then he has worked in the field of sophisticated and adaptive automation systems for IHC Systems, and later for Imtech Marine & Offshore BV. In 1997 he again joined IHC Systems as manager R&D, where the attention is focused on sophisticated automation, integrated bridges and training simulators for dredgers.

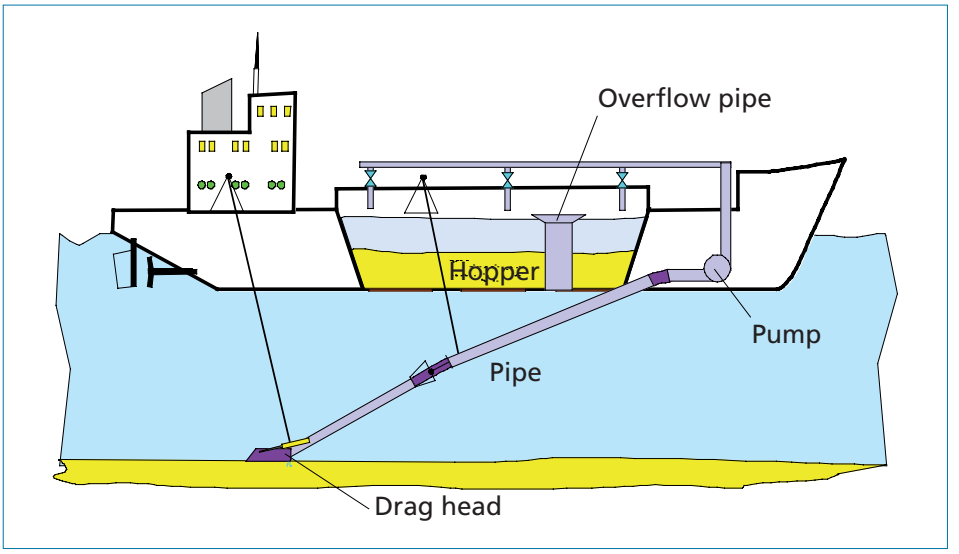

Figure 1. A schematic drawing of a hopper dredger.

Usually two crewmembers operate the ship. One is responsible for maneuvering the ship and determines the ship's speed. The other operator controls the excavation and storage process. This operator is mainly concerned with hoisting and lowering the pipes to prevent the draghead from being pulled under the ship. This demands a great deal of attention and leaves little time left for optimising the sedimentation process inside the hopper. Moreover the operator cannot look inside the hopper to see whether the settling process functions properly or whether the set-points need adjustment. One solution to this would be to install additional sensors in the hopper, but this requires considerable investments and maintenance.

The alternative presented here is a model-based approach. The model is used to predict the internal behaviour of the sand bed and the overflow losses. The model can be used for the following applications:

- Process monitoring; the operator is able to see if the sand bed is still growing and whether the overflow density is too high.
- Decision support; the model is used to predict the sedimentation behaviour in dependence on the set-points and suggest the best set-points on screen.
- Model predictive control; this controller optimises the whole dredging process, based on predictions of an internal model of the process.

The control objective of such a model predictive controller can be to minimise the integral dredging costs per m^3 of sand or maximise the production per time unit. At every sampling instant, for example, 5 minutes, the optimal future trajectory of the set-points is determined. Examples of the set-points are the dredge pump speed (incoming flow rate) or the height of the overflow pipe in the hopper. To determine the optimal trajectory, the model must be simulated over a finite time horizon up to 1000 times. This leaves an execution time of the model of less than 0.3 seconds. In the literature, a number of sedimentation models have been proposed [1], [7], [9], [11]. These models, however, cannot be used for real-time control or optimisation of the dredging process, because they are based on detailed modelling of the physical phenomena by using Partial Differential Equations (PDE) and thus contain too many uncertain parameters. Therefore, simplified and computationally efficient models are proposed here for the optimisation of the hopper sedimentation process. The objective of the model is to predict the sand bed height and the overflow density.

Prior to stating the modelling problem, the loading process is briefly described in more detail. This process shows three different phases:

List of Symbols

A	hopper area	k'_o	parameter for full overflow	v_s	settling velocity
g	acceleration due to gravity	$k_{\rho e}$	density decay factor in exponential model	v_{s0}	undisturbed settling velocity
h_b	height of the sand bed	$k_{\rho l}$	density slope in linear model	V_t	total hopper volume
b_{b0}	initial height of the sand bed	m_s	mass of the sand bed	β	exponent in settling velocity
h_m	height of the mixture layer	m_t	total hopper mass	ρ_i	incoming mixture density
h_o	height of the overflow pipe	$p_{1...12}$	parameters polynomial function	ρ_m	density of mixture above sand bed
h_t	total height of the hopper content	Q_i	incoming flow-rate	ρ_o	outgoing mixture density
h_w	height of the water layer	Q_{ms}	mixture soup flow-rate	ρ_q	quartz density
J	cost function for parameter estimation	Q_o	outgoing mixture flow-rate	ρ_s	density of sand bed
k_e	erosion parameter	Q_s	settling sand flow-rate	ρ_w	water density
k_o	parameter for free overflow	Q_w	water flow-rate		

- In the first phase, the height of the hopper content h_t is below the height of the overflow pipe h_o (see the list above for the definition of the symbols).
- The second phase starts when the hopper content height reaches the overflow pipe. The overflow pipe height stays constant, and therefore this phase is called the "constant-volume" phase. Typically, water or low-density mixture is flowing overboard in this phase.
- The third phase starts when the ship reaches its maximum draught. The overflow pipe is automatically lowered such that a constant hopper mass is maintained. This phase is called the "constant-tonnage" phase and the overflow losses are typically larger than in the constant-volume phase. This phase ends when the losses become so high that it is no longer economical to continue dredging.

The efficiency of the sedimentation process heavily depends on the type of soil and is influenced by the flow rate and density of the incoming mixture and the way the overflow pipe is controlled. An important factor in the optimisation of the dredging performance is the minimisation of the overflow losses.

This article is organised as follows: In the first section, the mass balance equations are given, followed by a simple model for the outgoing flow. Thereafter three different implementations of the overflow density are proposed and compared using data measured onboard a dredger with a hopper volume of 13,000 m^3 and on the test rig the *Schanulleke*. Finally the conclusions are presented based on the data.

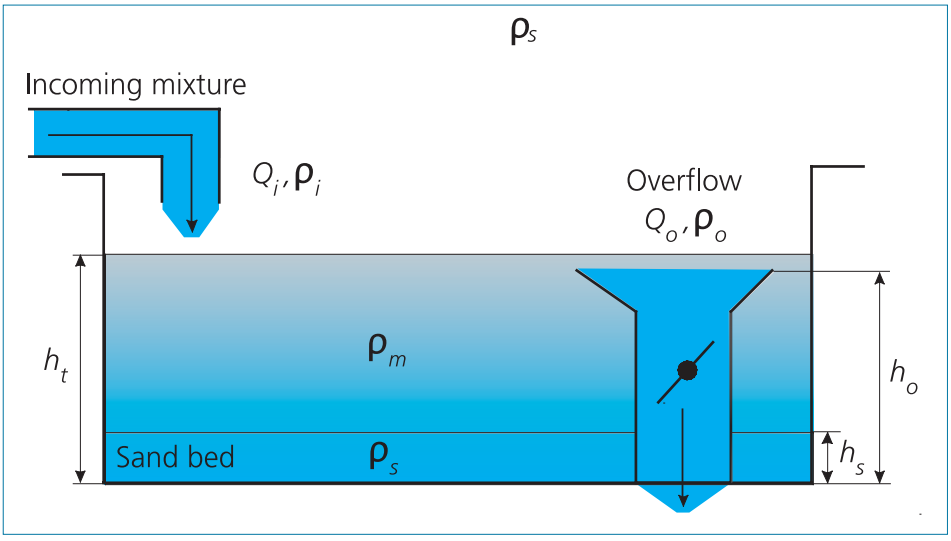

Figure 2. The sedimentation process in the hopper.

MASS-BALANCE EQUATIONS

The model must predict the sand bed height as well as the overflow density. For optimisation purposes the model must be as fast as possible. A model that meets this requirement is a one-dimensional (1D) approximation. Of course accuracy must be maintained and this was verified on the data of a ship and the data of a test rig (see below under "Ship Data").

The model has three state variables:
- the total mass in the hopper m_t,
- the total volume V_t of the mixture in the hopper, and
- the mass of the sand bed m_s.

While the first two states can be derived from online measurements (the ship draught and the height h_t respectively), the mass of the sand bed is not measurable. The flow-rate Q_i of the incoming mixture and the overflow height h_o are the manipulated inputs and the incoming mixture density ρ_i is considered in this context as a measured disturbance. The sedimentation dynamics are described by the following differential equations:

$$\begin{aligned} \dot{V}_t &= Q_i - Q_o \\ \dot{m}_t &= Q_i \rho_i - Q_o \rho_o \\ \dot{m}_s &= Q_s \rho_s . \end{aligned} \qquad (1)$$

The first two equations represent the volume and mass balance, respectively. The third equation gives the rate of sand sedimentation, where Q_s is the sand flow rate from the mixture layer to the sand layer and ρ_s is the sand density.

Gravity is the driving force of the flow Q_s.

A single grain settles with a velocity v_{s0}, while particles in a dense suspension have a lower settling velocity. Based on experiments, Richardson and Zaki [10] suggested an expression for the actual settling velocity, $v_s = v_{s0}(1 - C_m)^{\beta}$, where

$$C_m = \frac{\rho_m - \rho_w}{\rho_q - \rho_w}$$

is the volumetric concentration of the mixture.

In non-stagnant flow conditions where erosion might be important, the sedimentation velocity is computed by the difference between the settling flux and the erosion (pickup) flux. According to van Rhee [9] the final settling velocity becomes:

$$v_s = (1 - \mu) v_{s0} \left(\frac{\rho_q - \rho_m}{\rho_q - \rho_w} \right)^{\beta} \qquad (2)$$

where μ is a measure for erosion. This flow is in steady state considered to be equal to the overflow rate Q_o van Rhee [9] proposed the following quadratic dependency for μ:

$$\mu = min\left(\frac{Q_o^2}{k_e h_m^2}, 1 \right)$$

where $h_m = h_t - h_b$ is the mixture layer height.

The sedimentation process exhibits a discontinuity in density and velocity at the sand bed height $h_b(t)$, called a shock front. The evolution of the sand bed layer across the shock front follows from the conservation of mass:

$$\frac{\partial}{\partial_t} \iiint_V \rho \, dV = \iint_S \rho v_s \, dS$$

where V is the control volume, A is the area where mass is flowing in or out of the control volume and v_s is the settling velocity of the particles. In the 1D case presented here, this equation simplifies to:

$$\frac{d}{dt} \int_0^b \rho(h) \, dh = [\, \rho(h) \, v_s(h)]_0^b \qquad (3)$$

where the density $\rho(h)$, the velocity $v_s(h)$ are functions of the height h and b is a point well above the sand bed height h_b.

Splitting up the integral at the left-hand side, the results obtained were:

$$\frac{d}{dt} \left\{ \int_0^{h_b(t)} \rho(h) \, dh + \int_{h_b(t)}^{b} \rho(h) dh \right\} = (\rho_s - \rho_m) \frac{dh_b}{dt}. \qquad (4)$$

The right-hand side of (3) is the following:

$$[\, \rho(h) \, v_s(h)]_0^b = \rho_s . 0 - (- \rho_m \, v_s + \rho_w \, v_s) \qquad (5)$$

The first term is zero because the velocity of the particles in the sand layer is zero. The second term $-\rho_m v_s$ is the mass flux of the particles settling in the mixture. The third term $-\rho_w v_s$ is the mass flux of water flowing upward as a result of the settling particles. Combining (4) and (5) gives the following expression:

$$(\rho_s - \rho_m) \frac{dh_b}{dt} = (\rho_m - \rho_w) \, v_s . \qquad (6)$$

Substituting (2) into (6) leads to:

$$\frac{dh_b}{dt} = (1 - \mu) \, v_{s0} \frac{\rho_m - \rho_w}{\rho_s - \rho_m} \left(\frac{\rho_q - \rho_m}{\rho_q - \rho_w} \right)^{\beta}$$

Finally the expression for the sand flow rate follows from $Q_s = A \frac{dh_b}{dt}$:

$$Q_s = A(1 - \mu) \, v_{s0} \frac{\rho_m - \rho_w}{\rho_s - \rho_m} \left(\frac{\rho_q - \rho_m}{\rho_q - \rho_w} \right)^{\beta}$$

where A is the hopper area.

OVERFLOW RATE

The overflow process can operate in two different regimes. In the first regime, the outgoing mixture freely flows through the overflow pipe and the flow-rate Q_o is given by [4]:

$$Q_o = k_o \, max\,(h_t - h_o, 0)^{\frac{3}{2}}$$

where k_o is an uncertain parameter depending on the overflow pipe shape and circumference. In the second regime, the overflow pipe is full (because a valve inside the pipe is engaged, see Figure 2) and the following model must be used:

$$Q_o = k_o \sqrt{2 \, g \, max\,(h_t - h_o, 0)}.$$

Clearly, there is some uncertainty in the modelling of the overflow rate. Moreover, as a result of the model's switching nature, it is not straightforward to estimate its parameters.

To circumvent this uncertainty in the model tuning and validation, an estimate of the overflow rate based on the volume and input flow-rate measurements is used. This estimate is based on the discretised equation (1):

$$\bar{Q}_{o,k} = Q_{i,k} - \frac{1}{T_s} (V_{t,k+1} - V_{t,k}).$$

Here, the bar denotes that the variable is calculated, index k denotes the discrete time step and T_s is the sample time. As the volume measurement is noisy, an anti-causal first-order low-pass filter is first applied to this signal. The cut-off frequency was experimentally chosen at 0.001 Hz.

OVERFLOW DENSITY

The accurate prediction of the overflow density requires a model of the density profile in the mixture above the sand bed. The density is a decreasing function of the height above the sand, but the exact form of this function is uncertain and time varying.

Three models are proposed in this section:
- a linear model,
- an exponential model and
- a piece-wise constant (water-layer) model.

1. Linear Model

This model assumes that the mixture density decreases linearly in the upward direction. Under this assumption, the density $\rho(h)$ at a particular height h above the hopper bottom is given by:

$$\rho(h) = max(\rho_s - k_{pl}(h - h_b), \rho_w). \qquad (7)$$

The only parameter in this equation is the slope k_{pl}. It can be uniquely determined by considering the fact that the average mixture density ρ_m

$$\rho_m = \frac{m_t - m_s}{V_t - \frac{m_s}{\rho_s}} = \frac{\rho_s (m_t - m_s)}{V_t \rho_s - m_s} \qquad (8)$$

must equal the average of the density profile (7):

$$\rho_m = \frac{1}{h_m}\int_{h_b}^{h_t} max\,(\rho_s - k_{\rho l}\,(h - h_b), \rho_w)\,dh \quad (9)$$

with $h_m = h_t - h_b$. To solve (9) for $k_{\rho l}$, one needs to distinguish the two situations depicted in Figure 3.

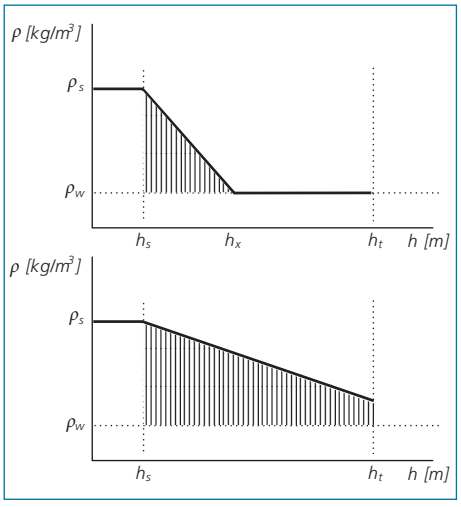

Figure 3. Two different situations with the linear density profile.

The top panel shows the situation in which the average mixture density ρ_m is so low that the mixture only reaches the height $h_b + h_x < h_t$. The integral in (9) then equals to:

$$\rho_m = \frac{1}{h_m}\left(\rho_w h_m + \frac{1}{2} h_x (\rho_s - \rho_w)\right)$$

from which is expressed:

$$h_x = \frac{2h_m (\rho_s - \rho_w)}{\rho_s - \rho_w} \quad (10)$$

and the slope is computed as:

$$k_{\rho l} = \frac{\rho_s - \rho_w}{h_x} = \frac{(\rho_s - \rho_w)^2}{2h_m(\rho_m - \rho_w)} \quad (11)$$

In the limit case for this situation, the indicated triangle spans the entire mixture layer. The substitution $h_x = h_m$ into (10) gives the limit condition for ρ_m:

$$\rho_m = \frac{1}{2}(\rho_w + \rho_s) \quad (12)$$

If $\rho_m > \frac{1}{2}(\rho_w + \rho_s)$, the integral in (9) includes the trapezoid, as shown in the bottom panel of Figure 3. The slope becomes:

$$k_{pl} = \frac{2\,(\rho_s - \rho_m)}{h_m} \quad (13)$$

Combining equations (11) and (13) yields the final equation for the slope:

$$k_{pl} = \begin{cases} \dfrac{2\,(\rho_s - \rho_m)}{h_m} & \text{for } \rho_m > \dfrac{1}{2}(\rho_w + \rho_s) \\ \dfrac{(\rho_s - \rho_w)^2}{2h_m(\rho_m - \rho_w)} & \text{otherwise.} \end{cases} \quad (14)$$

The overflow density is obtained by substituting $h = h_o$ into (7):

$$\rho_o = max\left(\rho_s - k_{pl}\,(h_o - h_b),\, \rho_w\right). \quad (15)$$

Equations (14) and (15) constitute the linear model for the overflow density ρ_o.

2. Exponential Model

This model assumes an exponentially decreasing function of the height above the sand layer (Figure 4).

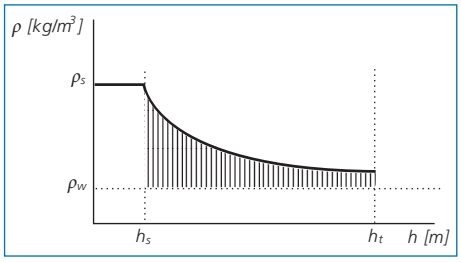

Figure 4. Density profile of the exponential model.

The density $\rho(h)$ at height h is given by:

$$\rho(h) = \rho_w + (\rho_s - \rho_w)e^{-k_{\rho e}\,(h - h_b)}. \quad (16)$$

The coefficient $k_{\rho e}$ can again be uniquely determined by considering the fact that the average mixture density ρ_m (8) must equal the average of the exponential profile:

$$\rho_m = \frac{1}{h_m}\int_{h_b}^{h_t} \rho_w + (\rho_s - \rho_w)e^{-k_{\rho e}\,(h - h_b)}\,dh.$$

Computing the integral, results in the equation:

$$\rho_m = \frac{\rho_s - \rho_w + \rho_w k_{\rho e} h_m - (\rho_s - \rho_w)e^{-k_{\rho e} h_m}}{h_m k_{\rho e}}$$

which can be re-arranged into:

$$1 - ak_{\rho e} = e^{\,bk_{\rho e}} \quad (17)$$

with

$$a = \frac{h_m\,(\rho_m - \rho_w)}{\rho_s - \rho_w} \quad \text{and} \quad b = -h_m.$$

Although this equation cannot be directly solved for $k_{\rho e}$ through algebraic manipulations it can come in the form $y = xe^x$, whose solution is $x = W(y)$, where W is the Lambert's W function [2].

First, multiply both sides of (17) by $\frac{b}{a}e^{\frac{b}{a} - bk_{\rho e}}$ to obtain the following equation:

$$\left(\frac{b}{a} - bk_{\rho e}\right)e^{\left(\frac{b}{a} - bk_{\rho e}\right)} = \frac{b}{a}e^{\frac{b}{a}}$$

whose solution is:

$$\frac{b}{a} - bk_{\rho e} = W\left(\frac{b}{a}e^{\frac{b}{a}}\right).$$

Finally express $k_{\rho e}$:

$$k_{\rho e} = \frac{1}{a} - \frac{1}{b}W\left(\frac{b}{a}e^{\frac{b}{a}}\right)$$

and substitute back for a and b:

$$k_{\rho e} = \frac{1}{h_m}\left[\frac{\rho_s - \rho_w}{\rho_m - \rho_w} + W\left(\frac{\rho_s - \rho_w}{\rho_w - \rho_m}e^{\frac{\rho_s - \rho_w}{\rho_w - \rho_m}}\right)\right]. \quad (18)$$

As the Lambert's W function only depends on one variable ρ_m, it can be easily approximated by a polynomial, in order to reduce the computation time. To make the approximated function independent of the parameters ρ_s and ρ_w, define:

$$f(k)\,W\left(-\frac{1}{k}e^{-\frac{1}{k}}\right)$$

where k = $\frac{\rho_m - \rho_w}{\rho_s - \rho_w}$ and $k \in (0,1]$. Function $f(k)$ can be accurately approximated by a 12th-degree polynomial:

$$f_p(k) = p_0 + p_1 k + \cdots + p_{12}k^{12}$$

where the coefficients are found by least-squares fitting. The overflow density is obtained by substituting $h = ho$ into (16):

$$\rho(h) = \rho_w + (\rho_s - \rho_w) e^{-k_{\rho e}(h - h_b)} \quad (19)$$

Equations (18) and (19) constitute the exponential model for the overflow density ρ_o.

3. Water-layer Model

The density profile above the sand layer is approximated by a two-layer (piece-wise constant) model (Figure 5). This model assumes that a thin water layer is formed on top of the mixture soup layer [7]. This layer is formed by an upward flow of water which is caused by the settling of the grains.

The displacement of a volume of grains downwards invokes the same volume of water flowing in the opposite direction.

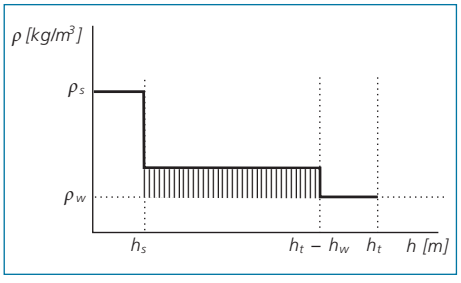

Figure 5. Density profile of the water-layer model.

The overflow rate Q_o is the sum of the water flow Q_w and the mixture soup flow Q_{ms}, (Figure 6). It is assumed that Q_w flowing out of the hopper equals the upward water flow at the bed height. The positive flow Q_w is directed upward and of the solids downwards (Figure 6). The water flow is equal to the flow of the solids through the mixture:

$$Q_w = Q_{solids}$$

where Q_{solids} is the volumetric flow of the grains (solids) in the mixture. Note that Q_{solids} is different from Q_s, because Q_s is the sand flow rate relative to the sand bed. And because this bed is rising the Q_s is different than Q_{solids}. The flow of solids through an area in the hopper is given by:

$$Q_{solids} = A_s v_s = A C_{ms} v_s$$

where A_s is the cross section area of the grains and C_{ms} is the volumetric concentration of the mixture soup. Using (2), this leads to the following expression for the water flow Q_w:

$$Q_w = A(1-\mu) v_{s0} \frac{\rho_m - \rho_w}{\rho_q - \rho_w} \left(\frac{\rho_q - \rho_m}{\rho_q - \rho_w} \right)^{\beta}. \quad (20)$$

For small Q_o, only pure water from the water layer is flowing out at the overflow. However, when Q_o becomes larger than Q_w, the mixture soup flow becomes nonzero:

$$Q_{ms} = max\,(Q_o - Q_w, 0). \quad (21)$$

The outgoing density ρ_o is given by the mixing of the two flows:

$$\rho_o = \frac{\rho_{ms} Q_{ms} + \rho_w Q_w}{Q_{ms} + Q_w} \quad (22)$$

The density of the mixture soup can be computed as $\rho_{ms} = (h_m \rho_m - h_w \rho_w)/(h_m - h_w)$.

However, as the water-layer height h_w is not known, an additional assumption must be made. It is assumed that the water layer is very thin and hence the mixture soup density ρ_{ms} approximately equals the total mixture density ρ_m. Substituting $\rho_{ms} = \rho_m$ into (22), the overflow density is given by:

$$\rho_o = \frac{(\rho_m - \rho_w) Q_{ms}}{Q_{ms} + Q_w} + \rho_w. \quad (23)$$

Equations (20), (21) and (23) constitute the water-layer model for the overflow density ρ_o.

PARAMETER CALIBRATION AND MODEL VALIDATION

The models contain unknown parameters which must be calibrated. Some parameters depend on the ship's configuration and geometry and the rest on the soil type. The geometric parameters such as A and k_o are calibrated once and are constant for all dredging cycles. The soil type dependent parameters are ρ_s, v_{so}, k_e, h_{bo} and β, where h_{b0} is the initial bed height before dredging.

During dredging, the soil type is not exactly known and is time varying, therefore these parameters must be adapted during operation. The only way of doing this is by estimating the parameters from the available measurements on board of the dredger.

Data is used from a test rig, which is a scaled down version of the suction dredger, *Antigoon* [8]. Although the test rig shows the calibration results on a scaled down version of a hopper, it does not guarantee that the models perform similarly when used on the actual ship. This performance is tested with data from a dredger with a hopper volume of 13,000 m^3. Models are used to predict total mass in the hopper, which is the only available measurement related to the overflow density. If the model is predicting the mass correctly, the model for the overflow density is also valid on the actual ship.

1. Parameter Calibration based on Data from Test Rig

1. Available Measurements

The following measurements are available:

- inlet pipe: the density ρ_i and the flow-rate Q_i
- hopper: the height of the hopper content h_t and the height of the overflow pipes h_o
- overflow pipe: the density ρ_o and the flow-rate Q_o
- inside mixture: Conductivity Concentration Meters (CMM) measure the mixture density at discrete heights with a spacing of 20 cm and a radioactive concentration fork performs an accurate measurement of the density at one location, which is varied in time.

These CCM measurements are not very accurate, but sufficient to indicate the height of the sand bed h_b. For one loading cycle, approximately 14 measurements of the bed height are obtained. Note that there is no hopper mass measurement available in the test rig.

2. Cost Function

The predicted model output is generated by dynamic simulation using an Ordinary Differential Equation (ODE) solver. The result is compared to the measurements.

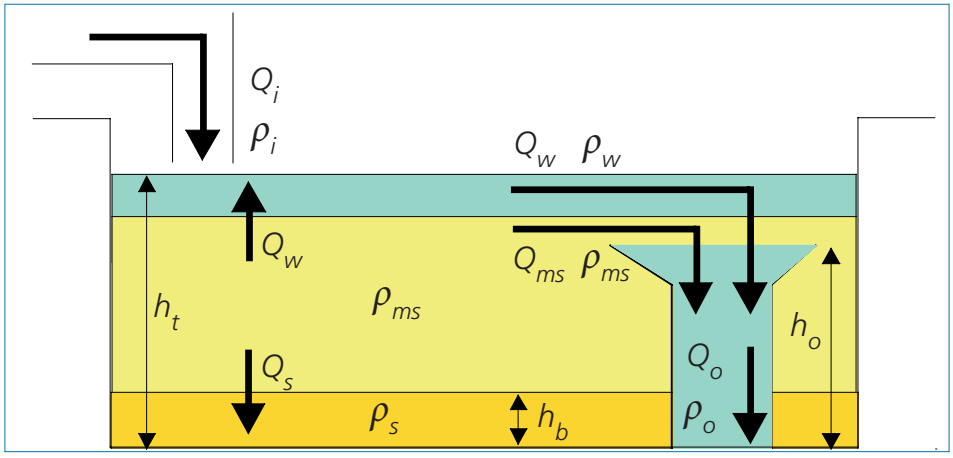

Figure 6. A schematic of the water-layer model.

The following cost function must be minimised:

$$J = \min_{\Theta} \left(\frac{a}{N_1} \sum_{k=1}^{N_1} (\rho_o(k,\Theta) - \rho_o^*(k))^2 + \frac{1-a}{N_2} \sum_{k'=1}^{N_2} (h_b(k',\Theta) - h_b^*(k'))^2 \right)$$

subject to

$$\Theta_{min} \le \Theta \le \Theta_{max}$$

where N_1 is the number of samples of the first criterion, N_2 is the number of samples of the second criterion, $\Theta = [\, v_{s0}\, k_e\, \rho_s\, h_{b0}\, \beta \,]^T$ is the parameter vector, a is a weight, $\rho_o(k,\Theta)$ and $hb(k',\Theta)$ are the model outputs from the ODE solver and the * denotes a measured variable.

Note that the number of measurement samples of ρ_o and h_b are different. The ρ_o is measured with a sample rate of one second and there are approximately $N_1 = 800$ measurements taken in each cycle. The bed height h_b is limited to $N_2 = 24$ samples because of the discrete placement of the CCM sensors. In practice there are at most 14 samples to work with.

2. Parameter Calibration and Validation based on Data from Ship

1. Available Measurements

On the actual ship the following quantities are measured:

- inlet pipe: the density ρ_i and the flow-rate Q_i
- hopper: the height h_t and the height of the overflow pipes h_o
- hull: the draught of the ship with pressure sensors, from this data the hopper mass m_t is derived.

No sensors are installed inside the hopper and in the overflow pipes, therefore the density ρ_o and the flow-rate Q_o are not measured. The measurement of the total mass is used to validate the prediction of ρ_o.

2. Cost Function

The parameter estimation for the ship data is different, because the sand bed height and the outgoing density are not measured. This is a more complex estimation problem, because there is less measurement information of the process. It is therefore desirable to reduce the number of parameters to estimate as much as possible. The parameter β, has a small influence on the measured mass m_t and is kept constant $\beta = 4$. Furthermore the h_{b0} is

$$J = \min_{\Theta} \frac{1}{N} \sum_{k=1}^{N} (m_t(k,\Theta) - m_t^*(k))^2$$

calculated beforehand. The cost function to minimise is in this case the following: with $\Theta = [v_{so}\ k_e\ \rho_s]^T$. Sensitivity analysis shows that this limited set of parameters is most suitable for the estimation. The initial bed height h_{b0} is calculated from the initial mass and volume. Assuming that initially the hopper load is composed of a sand layer with the density ρ_s and a water-layer, the initial state of the sand layer:

$$m_s(0) = \rho_s \left(\frac{m_t(0) - V_t(0)\rho_w}{\rho_s - \rho_w} \right).$$

The initial bed height follows from:

$$h_{b0} = \frac{m_s(0)}{\rho_s A}.$$

3. Nonlinear Optimisation

As the model outputs are nonlinear in the parameters, the parameter estimation problem has to be solved by nonlinear optimisation. Several nonlinear global optimisation methods are available, such as multi-start local optimisation, random search, simulated annealing, genetic algorithms and pattern search methods [3], [5], [6]. Finding a global minimum is computationally expensive and may result in a local minimum.

The goal here is to use the parameter estimation in an online application; therefore multi-start local minimisation (gradient-based approach) is not suitable because of the long estimation time (several hours). A pattern search algorithm for the estimation of the parameters [6] is used. This pattern search algorithm shows better performance in terms of computational time and is less sensitive to local minima than the gradient-based approach.

4. Results for the Test Rig Data

Thirty optimisation runs are performed with each model, where the parameters are randomly initialised within the ranges of Table I. The performance in terms of predicting the bed height is similar for the three models when solely looking at the least squares error. The differences are found in the beginning of the cycle: the algorithm finds 3 different initial values for each model of the bed heights. Based on the cost function, the exponential model gives the best prediction (see Table I). This table shows also the estimated parameters for the three models.

Figure 7 gives the output density for each model and Figure 8 the bed height. Both figures show also the measured data. The exponential model shows the best prediction of the output density. The water-layer model shows similar performance with the exception of the beginning of the cycle.

The particle size distribution is known for the test rig data. The mean particle size is between 0.11 and 0.14 mm. For this particle

Table I. Results of the parameter estimation of the test rig data.

Parameters		Range	Models		
			Linear	Exponential	Water layer
v_{s0}	[mm/s]	0.1···400	7.7	6.1	14
k_e	[-]	0.01···1	0.15	0.17	0.14
ρ_s	[kg/m^3]	1750···1875	1800	1800	1900
h_{b0}	[m]	0.1···0.8	0.53	0.55	0.47
β	[-]	3.5···5	5	5	5
J	[-]		1.5	3.1	4.0

Table II. Least squares error of the training and validation cycles, exponential model.

Validation cycle	Training Cycle		
	5	8	9
5	$3.7{\cdot}10^{-4}$	$4.7{\cdot}10^{-4}$	$3.4{\cdot}10^{-3}$
8	$3.7{\cdot}10^{-4}$	$2.9{\cdot}10^{-4}$	$2.1{\cdot}10^{-3}$
9	$9.0{\cdot}10^{-4}$	$1.1{\cdot}10^{-3}$	$2.7{\cdot}10^{-3}$

size according to Stokes the undisturbed settling velocity is between 8 and 16 mm/s. Table I shows that the parameter vs0 is in the same order of magnitude for all the models, so the physical meaning of the parameter is preserved.

RESULTS FOR THE SHIP DATA

Data of 12 dredging cycles are available for testing the models. The results for three cycles, randomly selected from the available data set, are shown here. For each model, 45 optimisation runs are performed on each cycle, where the parameters are randomly initialised within the ranges:

$$V_{s0} \in [1 \quad 400] \quad \text{mm/s}$$
$$k_e \in [0.1 \quad 55] \quad -$$
$$\rho_s \in [1700 \quad 2400] \quad \text{kg/m}^3$$

Not every optimisation run is successful; therefore the 25 best runs for each cycle and each model are selected for the analysis given here. The optimal parameters are given by the median values of the 25 runs. For all cycles and models, an optimal parameter vector Θ is found. These vectors are used to validate the models by predicting the total mass of the other cycles than the training cycle. The results are summarised in Tables II, III and IV, for the exponential, linear and water-layer model, respectively. The least squares error of the training results is on the diagonal and the validation results are given by the other elements. Note that the validation errors are in the same order of magnitude as the training errors. This indicates that no over fitting takes place and that the models describe the process instead of fitting the data.

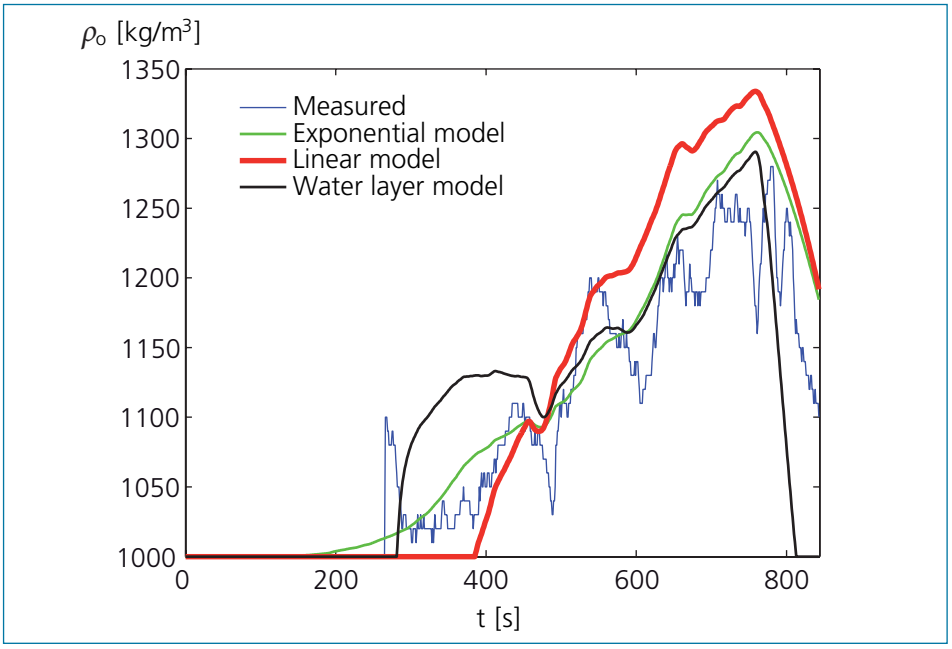

Figure 7. Comparison of the simulated output density of the three models and the measured test rig data.

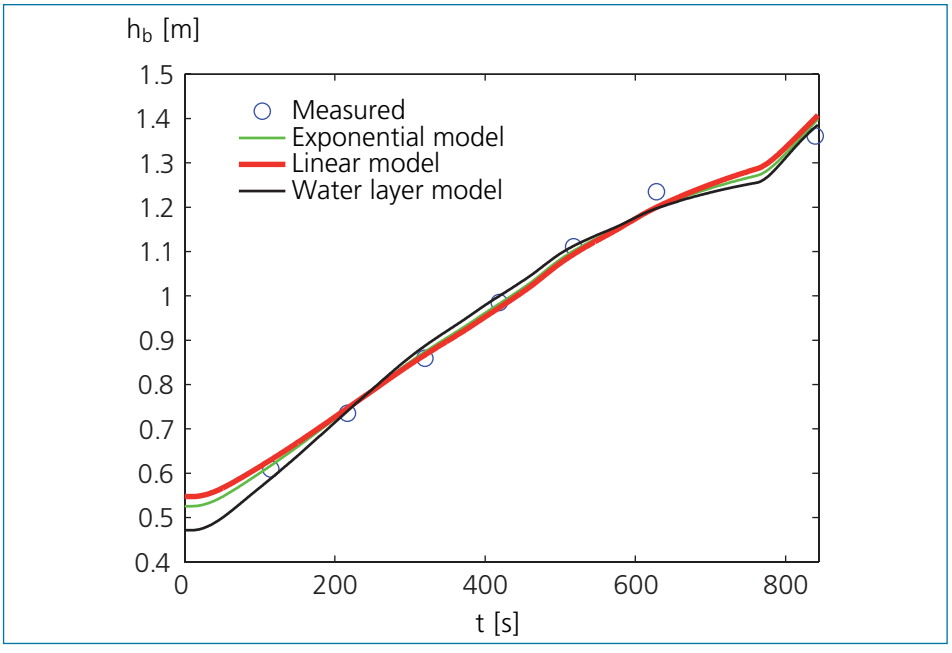

Figure 8. Comparison of the simulated sand bed height of the three models and measured test rig data.

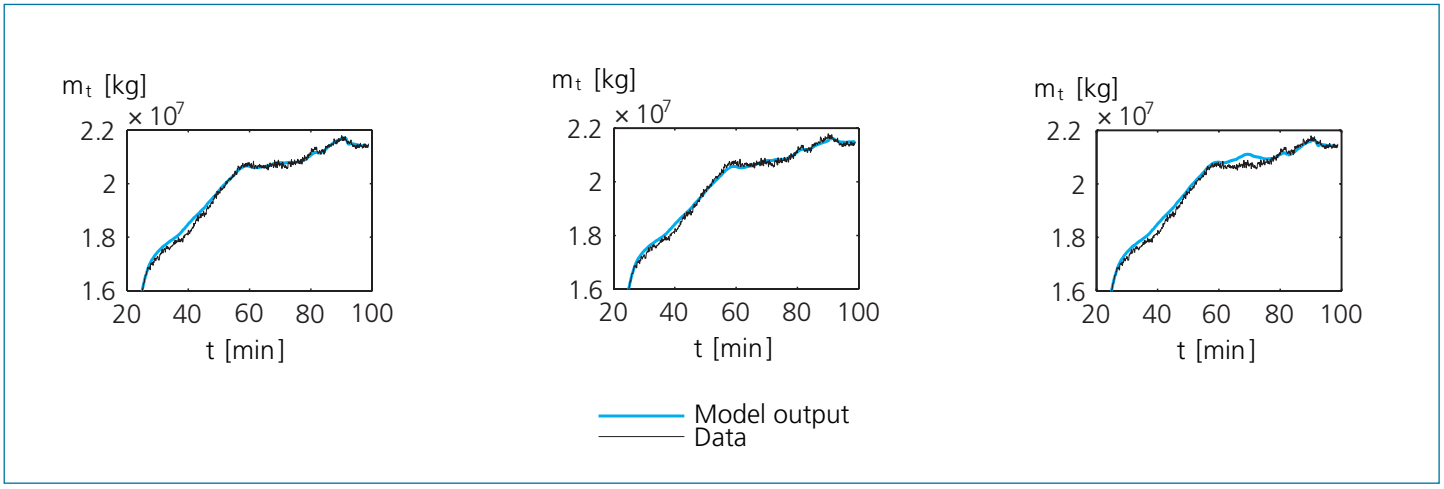

Figure 9. Training results for cycle 8: Left, exponential model; center, water-layer model; right, linear model.

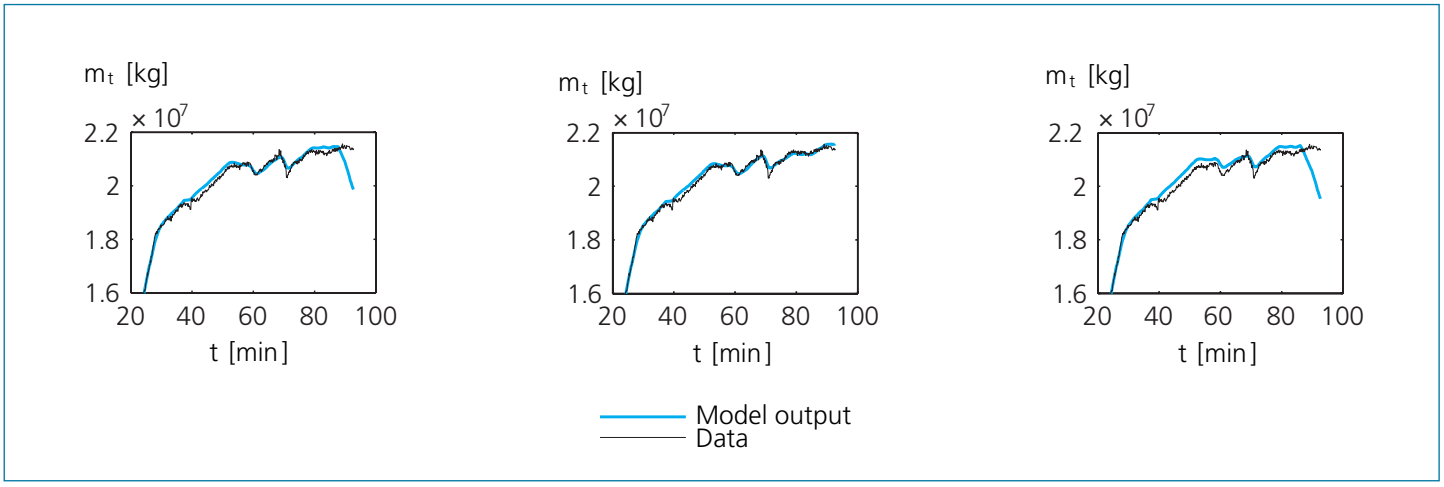

Figure 10. Validation results for cycle 9 with parameters (cycle 8): Left, exponential model; center, water-layer model; right, linear model.

Figure 9 shows the prediction of the total hopper mass by the 3 models for the training data and Figure 10 for the validation data. This last figure shows cycle 9 with the parameters calibrated on cycle 8.

Figures 9 and 10 also show that the linear model has very poor performance in the middle of the data sequence. This behaviour exists in all the cycles. Clearly the linear model is not accurate enough and underestimates the overflow density in the second and the third phase.

The least squares error of Tables II and III reveal that the water-layer model (Table IV) is the best model. This is also illustrated in the scatter plots in Figure 11 of the exponential and the water-layer model. Moreover Figure

Table III. Least squares error of the training and validation cycles, linear model.

Validation cycle	Training Cycle		
	5	8	9
5	$7.7 \cdot 10^{-4}$	$1.0 \cdot 10^{-3}$	$8.9 \cdot 10^{-4}$
8	$5.9 \cdot 10^{-4}$	$5.6 \cdot 10^{-4}$	$6.6 \cdot 10^{-4}$
9	$6.4 \cdot 10^{-4}$	$1.4 \cdot 10^{-3}$	$5.0 \cdot 10^{-4}$

Table IV. Least squares error of the training and validation cycles, water-layer model.

Validation cycle	Training Cycle		
	5	8	9
5	$3.2 \cdot 10^{-4}$	$1.1 \cdot 10^{-3}$	$1.0 \cdot 10^{-3}$
8	$5.6 \cdot 10^{-4}$	$2.5 \cdot 10^{-4}$	$3.0 \cdot 10^{-4}$
9	$6.4 \cdot 10^{-4}$	$2.5 \cdot 10^{-4}$	$2.1 \cdot 10^{-4}$

Table V. Results estimation of the exponential model on three different cycles.

Cycle	v_{s0}	k_e	ρ_s	J
5	0.019	12	1980	$3.7 \cdot 10^{-4}$
8	0.020	9	1959	$2.9 \cdot 10^{-4}$
9	0.021	2.25	2055	$2.7 \cdot 10^{-3}$

Table VI. Results estimation of the linear model on three different cycles.

Cycle	v_{s0}	k_e	ρ_s	J
5	0.015	55	1986	$7.7 \cdot 10^{-4}$
8	0.0154	55	1958	$5.6 \cdot 10^{-4}$
9	0.0144	16	1971	$5.0 \cdot 10^{-4}$

Table VII. Results estimation of the water-layer model on three different cycles.

Cycle	v_{s0}	k_e	ρ_s	J
5	0.12	3.6	2116	$3.2 \cdot 10^{-4}$
8	0.18	2.6	2145	$2.5 \cdot 10^{-4}$
9	0.12	3.4	2059	$2.1 \cdot 10^{-4}$

10 shows a larger error for the exponential model at the end of the cycle. The sand bed height in the exponential model rises too fast and reaches the overflow height at the end of the cycle. This gives a large increase in the overflow density which results in a large decrease in the hopper mass.
The calibrated parameters in each cycle are shown in the Tables V, VI and VII.

These tables show that the parameters have a similar order of magnitude.
The water-layer model gives the smallest least square error *(J)* and the best validation results. The parameters estimated for the water-layer model differ significantly from the other two, especially when considering the parameters k_e and v_{s0}.

CONCLUSIONS

Three different models are proposed to predict the outgoing mixture density and bed height in the hopper. The models are deployed in an online optimiaation strategy such as a model predictive controller, therefore models were developed such that the simulation time is short.
The parameters are calibrated using least squares optimisation on test rig data and on real ship data. The ship data are used to validate the models by calibrating the parameters on one cycle and predicting the total mass on the other cycles. This resulted in the following conclusions.

The test rig data show that the three models have similar performance, but the exponential model gives the best fit.
The predicted parameter v_{s0} is in the same range following the theory of Stokes for all three models. This means that although simplified models were used the parameters still have physical meaning.

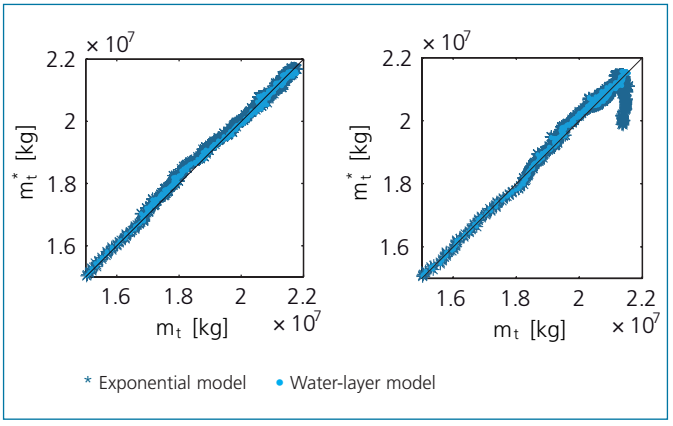

Figure 11. Scatter plots of the two best models (cycle eight), the training results (left) and the validation results (right).

When the models are used for the prediction of the hopper mass of the ship, the linear model performs poorly and is therefore rejected. It underestimates the overflow losses halfway the overflow phase. This model is not suitable for the model predictive controller because it is not accurate enough. The exponential and the water-layer models perform similarly on the training data, but the validation shows that the water-layer model is more accurate. The water layer model has a simulation time of less then 0.2 seconds and is therefore suitable for the use in an online optimisation system with a sample time of several minutes. This simulation time is an upper bound and will be less if the controller code is optimised for speed.

The predicted value for v_{s0} for these two models differs by a factor of 10. This indicates that the water-layer model predicts heavier sand than the exponential model. It is not possible to tell which of the two models is correct, because no information is available on the soil type. The water-layer model will be used for our model predictive controller.

REFERENCES

[1] Camp, T. (1946). "Sedimentation and the design of settling tanks". *Trans. ASCE, 895-936.*

[2] Corless, R.; Gonnet, G.; Hare, D.; Jeffrey, D. and Knuth, D. (1996). "On the Lambert W Function". *Advances in Computational Mathematics 5,* 329-359.

[3] Eglese, R. (1990). "Simulated annealing: A tool for operations research". *European Journal of Operational Research 46*, 271-281.

[4] Franzini, J. (1997). *Fluid Mechanics with Engineering Applications.* The McGraw-Hill Companies, Inc. New York.

[5] Goldberg, D. (1989). *Genetic Algorithms in Search, Optimization and Machine Learning.* Addison-Wesley, Reading, Massachusetts.

[6] Lewis, R. and Torczon, V. (1999). "Pattern Search Algorithms for Bound Constrained Minimization". *SIAM Journal on Optimization 9 (4)*, 1082-1099.

[7] Ooijens, S. (1999). "Adding Dynamics to the Camp Model for the Calculation of Overflow Losses". *Terra et Aqua* (76), 12-21.

[8] Ooijens, S., de Gruijter, A., Nieuwenhuijzen, A. and Vandycke, S. (2001). "Research on hopper settlement using large-scale modeling". *Proceedings CEDA Dredging Days 2001*, pp. 1-11.

[9] van Rhee, C. (2002). "On the sedimentation process in a Trailing Suction Hopper Dredger". PhD thesis, TU Delft, the Netherlands.

[10] Richardson, J. and Zaki, W. (1954). "Sedimentation and Fluidisation: Part I". *Transactions of the Institution of Chemical Engineers* 32, 35-53.

[11] Yagi, T. (1970). "Sedimentation effects of soil in hopper". *Proceedings of WODCON 1970.*